Supplementary Information

Low Lattice Thermal Conductivity in $Pb_5Bi_6Se_{14}$, $Pb_3Bi_2S_6$, and $PbBi_2S_4$: Promising Thermoelectric Materials in the Cannizzarite, Lillianite, and Galenobismuthite Homologous Series

Michihiro Ohta[1,2], Duck Young Chung[1], Masaru Kunii[2], Mercouri G. Kanatzidis[1,3]

[1]Materials Science Division, Argonne National Laboratory, Argonne, Illinois 60439, USA

[2]Energy Technology Research Institute, National Institute of Advanced Industrial Science and Technology (AIST), Tsukuba, Ibaraki 305-8568, JAPAN

[3]Department of Chemistry, Northwestern University, Evanston, Illinois 60208, USA

*Corresponding Author

E-mail: m-kanatzidis@northwestern.edu (M.G.K)

The density (d) of the sintered compacts is summarized in **Table S1**. The theoretical density was calculated from lattice parameters (**Table 1**). The room-temperature Hall coefficient (R_H) of the sintered compacts of $Pb_5Bi_6Se_{14}$, $Pb_3Bi_2S_6$, and $PbBi_2S_4$ is shown in **Table S2**. The thermal diffusivity (D) and heat capacity (C_P) of the $Pb_5Bi_6Se_{14}$, $Pb_3Bi_2S_6$, and $PbBi_2S_4$ sintered compacts are shown in **Figures S1** and **S2**, respectively. The scanning electron microscopy micrographs of three sintered compacts of different sizes were observed on the fractured sections parallel to the pressure direction in each system and are shown in **Figure S3–S5**.

Table S1. Density (d) of the sintered compacts of $Pb_5Bi_6Se_{14}$, $Pb_3Bi_2S_6$, and $PbBi_2S_4$.

Sample	Sintered d (g cm^{-3})	Theoretical d (g cm^{-3})
$Pb_5Bi_6Se_{14}$	7.79	7.84
$Pb_3Bi_2S_6$	7.09	7.10
$PbBi_2S_4$	7.11	7.14

Table S2. Room-temperature Hall coefficient (R_H) of the sintered compacts of $Pb_5Bi_6Se_{14}$, $Pb_3Bi_2S_6$, and $PbBi_2S_4$.

Sample	R_H (10^{-8} m^3 C^{-1})
$Pb_5Bi_6Se_{14}$	−12.9
$Pb_3Bi_2S_6$	−5.15
$PbBi_2S_4$	−13.6

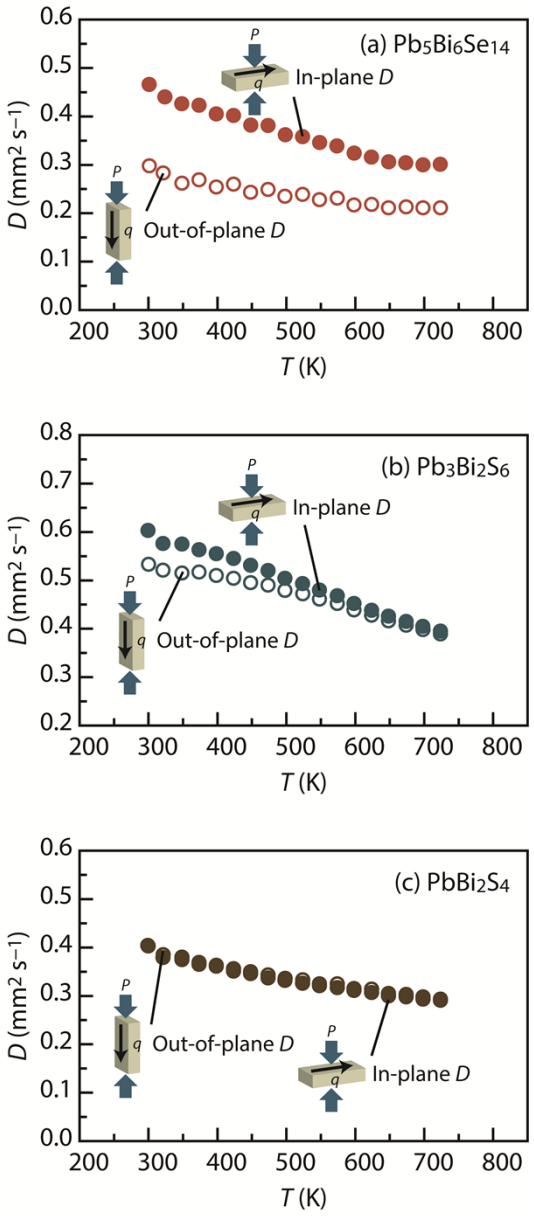

Figure S1. Temperature dependence of the thermal diffusivity (D) for sintered compacts of (a) $Pb_5Bi_6Se_{14}$, (b) $Pb_3Bi_2S_6$, and (c) $PbBi_2S_4$ measured perpendicular (in-plane) and parallel (out-of-plane) to the pressing direction.

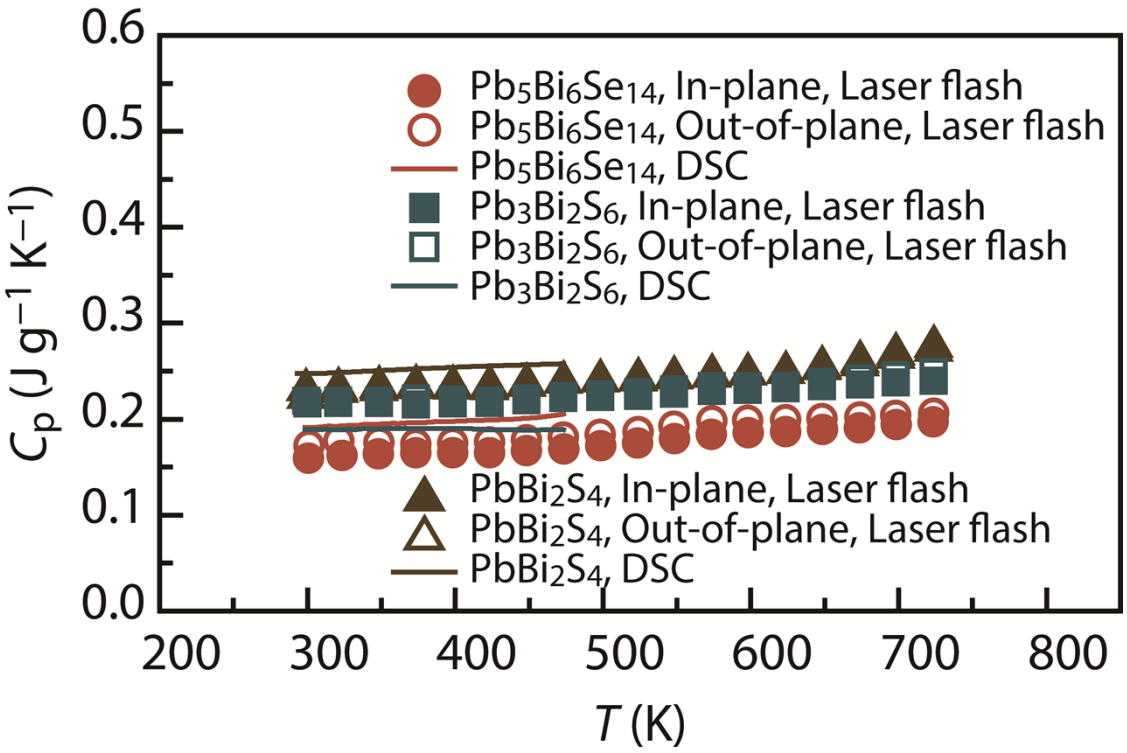

Figure S2. Temperature dependence of the heat capacity (C_P) of the sintered compacts of $Pb_5Bi_6Se_{14}$, $Pb_3Bi_2S_6$, and $PbBi_2S_4$.The heat capacity was indirectly derived using standard sample by using laser flash diffusivity method. The heat capacity was also measured using a differential scanning calorimetry (DSC).

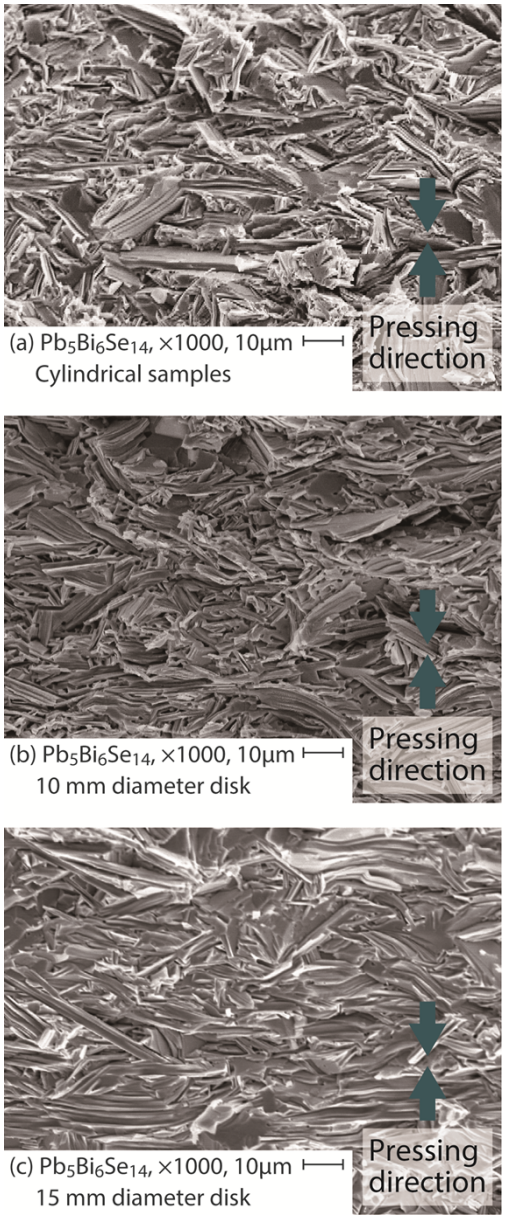

Figure S3. Scanning electron microscopy micrographs of the fractured section for the three $Pb_5Bi_6Se_{14}$ sintered compacts with different sizes; (a) cylindrical sample of ~10 mm diameter × ~11 mm length, (b) disk of ~10 mm diameter × ~2 mm thickness, and (c) disk of ~15 mm diameter × ~2 mm thickness. The samples were fractured parallel to the pressing direction.

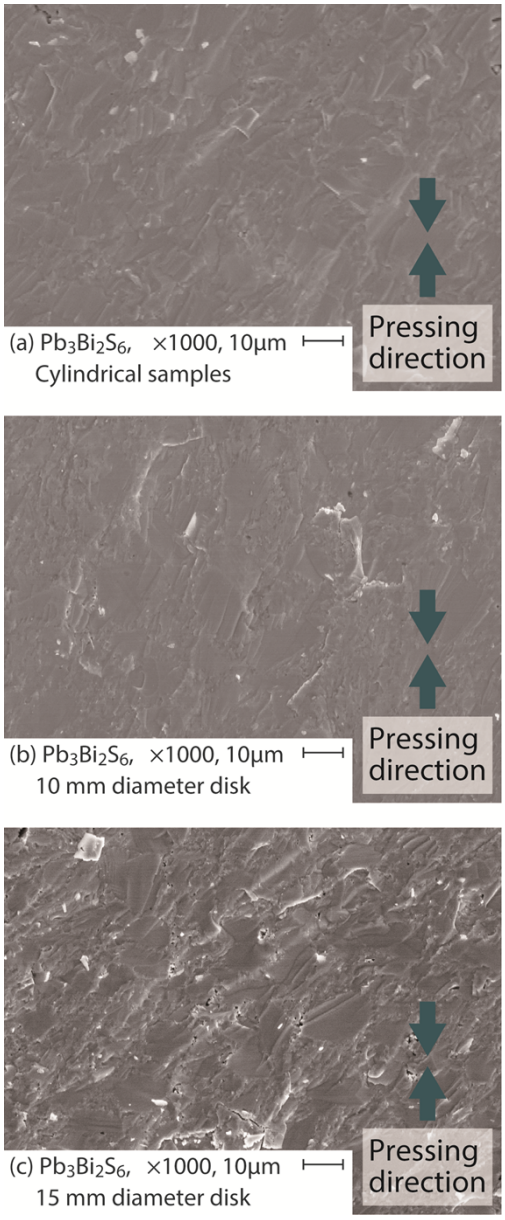

Figure S4. Scanning electron microscopy micrographs of the fractured section for the three $Pb_3Bi_2S_6$ sintered compacts with different sizes; (a) cylindrical sample of ~10 mm diameter × ~11 mm length, (b) disk of ~10 mm diameter × ~2 mm thickness, and (c) disk of ~15 mm diameter × ~2 mm thickness. The samples were fractured parallel to the pressing direction.

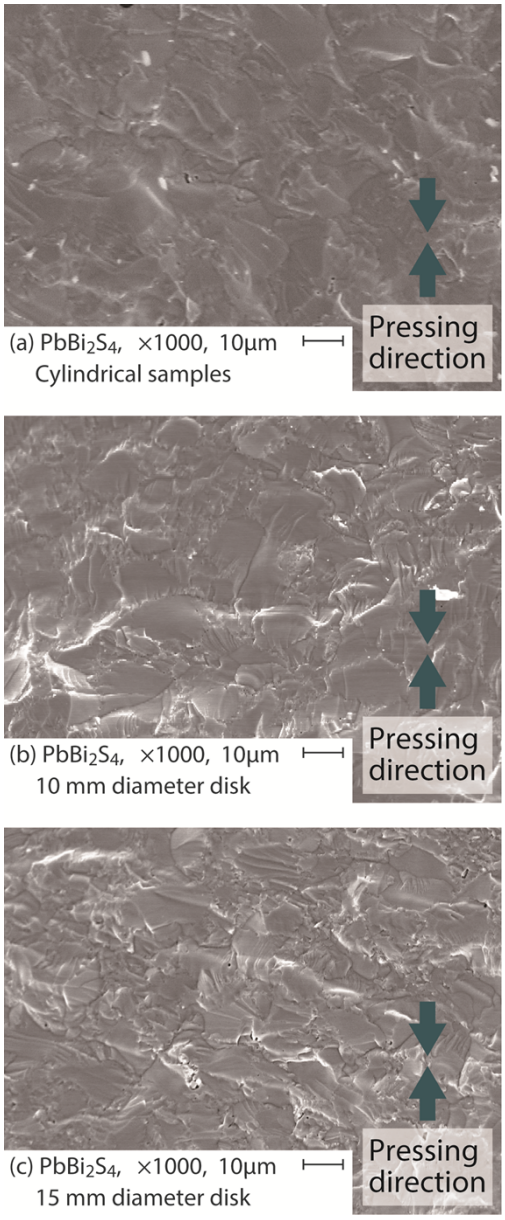

Figure S5. Scanning electron microscopy micrographs of the fractured section for the three $PbBi_2S_4$ sintered compacts with different sizes; (a) cylindrical sample of ~10 mm diameter × ~11 mm length, (b) disk of ~10 mm diameter × ~2 mm thickness, and (c) disk of ~15 mm diameter × ~2 mm thickness. The samples were fractured parallel to the pressing direction.